Phys Chem Minerals (2003) 30: 147–156
DOI 10.1007/s00269-003-0301-y

ORIGINAL PAPER

K. Litasov · E. Ohtani

Stability of various hydrous phases in CMAS pyrolite-H_2O system up to 25 GPa

Received: 9 September 2002 / Accepted: 11 January 2003

Abstract We carried out a series of melting experiments with hydrous primitive mantle compositions to determine the stability of dense hydrous phases under high pressures. Phase relations in the CaO–MgO–Al_2O_3–SiO_2 pyrolite with ~2 wt% of water have been determined in the pressure range of 10–25 GPa and in the temperature range between 800 and 1400 °C. We have found that phase E coexisting with olivine is stable at 10–12 GPa and below 1050 °C. Phase E coexisting with wadsleyite is stable at 14–16 GPa and below 900 °C. A superhydrous phase B is stable in pyrolite below 1100 °C at 18.5 GPa and below 1300 °C at 25 GPa. No hydrous phases other than wadsleyite are stable in pyrolite at 14–17 GPa and 900–1100 °C, suggesting a gap in the stability of dense hydrous magnesium silicates (DHMS). We detected an expansion in the stability field of wadsleyite to lower pressures (12 GPa and 1000 °C). The H_2O content of wadsleyite was found to decrease not only with increasing temperature but also with increasing pressure. The DHMS phases could exist in a pyrolitic composition only under the conditions present in the subducting slabs descending into the lower mantle. Under the normal mantle and hot plume conditions, wadsleyite and ringwoodite are the major H_2O-bearing phases. The top of the transition zone could be enriched in H_2O in accordance with the observed increase in water solubility in wadsleyite with decreasing pressure. As a consequence of the thermal equilibration between the subducting slabs and the ambient mantle, the uppermost lower mantle could be an important zone of dehydration, providing fluid for the rising plumes.

Keywords High pressure · High temperature · CMAS pyrolite · Mantle · DHMS phases · Hydrous conditions

K. Litasov (✉) · E. Ohtani
Institute of Mineralogy, Petrology and Economic Geology,
Tohoku University, Aoba-ku, Sendai, 980-8578, Japan
Tel.: +81-22-2176666
Fax: +81-22-2176675
e-mail: klitasov@ganko.tohoku.ac.jp

Introduction

Experimental studies of hydrous systems under mantle pressures suggested the existence of several dense hydrous phases (e.g., Ringwood and Major 1967; Gasparik 1993; Ohtani et al. 2000). Accordingly, the major hydrous phases in pyrolite compositions with increasing pressure should be represented by serpentine, chlorite and so-called dense hydrous magnesium silicate (DHMS) phases: phase A, phase E, superhydrous phase B (phase C) and phase G (D/F) (Mysen et al. 1998; Frost 1999; Ohtani et al. 2000). All these phases are stable at temperatures below 1300 °C. Wadsleyite and ringwoodite in the transition zone could hold a significant amount of H_2O at the elevated temperatures (Inoue et al. 1995; Kohlstedt et al. 1996). The nominally anhydrous phases, Mg-perovskite, Ca-perovskite and ferropericlase, in the lower mantle could also contain some H_2O (Murakami et al. 2002; Bolfan-Casanova et al. 2002). Most of the hydrous phases were synthesized via a simple silicate–water system (e.g., Frost 1999; Ohtani et al. 2000; Stalder and Ulmer 2001) or under water–saturated conditions (Kawamoto et al. 1995), whereas data for natural systems with a low amount of water are restricted.

Here we report results for a CMAS pyrolite composition with ~2 wt% H_2O at pressure ranging from 10 to 25 GPa, thereby providing new data on the stability of hydrous phases in a system with a low water content, which is closer to that observed in nature. The study is focused also on the water solubility, the compositional variations in coexisting phases and water transport and storage in the mantle.

Experimental

Phase relations and melt compositions in the CMAS pyrolite with 2 wt% of H_2O were determined at 10–25 GPa and the temperature range from 800 to 1400 °C. The starting materials (Table 1) were based on the anhydrous primitive mantle composition (Jagoutz

Table 1 Composition of starting materials. *PM* = the model primitive mantle composition proposed by Jagoutz et al. (1979) is simplified to four components, CaO, MgO, Al_2O_3 and SiO_2; according to the procedures of O'Hara (1968)

	SiO_2	Al_2O_3	MgO	CaO	H_2O	Total
PM + 2% H_2O	45.15	5.20	43.46	4.19	2.00	100

et al. 1979) estimated from spinel peridotite nodules and simplified to the four-component system CaO–MgO–Al_2O_3–SiO_2, following the procedures of O'Hara (1968). It should be noted that model primitive mantle composition by Jagoutz et al. (1979) is close to different pyrolite models (e.g., Ringwood 1975; McDonough and Sun 1995), therefore we refer to this composition as being a pyrolite.

The hydrous composition was prepared by adding $Mg(OH)_2$ to the synthetic mineral mixtures and adjusting the proportion of MgO. Additional details about the preparation of the starting material were described by Asahara and Ohtani (2001).

Experiments were conducted using a Kawai (MA8) multianvil system compressed by a cubic guide block in the 1000- and 3000-ton presses at the Tohoku University. The truncated edge length of the WC anvils was 3.5 mm for the 1000-ton press and 2.0 mm for the 3000-ton press. Platinum capsules were used as the sample containers. Semisintered zirconia was used as the pressure medium, and a cylindrical $LaCrO_3$ heater was used for the heating. Temperature was measured with a W3%Re–W25%Re thermocouple. The schematic cross-sections of the sample assemblies used in the experiments are shown in Litasov and Ohtani (2002).

System pressures were calibrated at 1600–2000 °C by bracketing the $\alpha-\beta$ and $\beta-\gamma$ phase boundaries of Mg_2SiO_4 (Morishima et al. 1994; Suzuki et al. 2000). The pressure uncertainty was determined to be within 1 GPa. The estimated uncertainties of the temperature are shown in Table 2. The temperature gradient across the charge was found to be less than 20–30 °C, which is the extrapolation from experiments at 4–8 GPa, where we can estimate temperature gradient at the temperature range by using two-pyroxene equilibria (Gasparik 1996; Asahara and Ohtani 2001).

Mineral compositions were analyzed by an electron microprobe under the accelerating potential of 15-kV and 10-nA specimen current. The phases were also identified by a micro-area X-ray powder diffractometer (MacScience M18XCE) and a micro-Raman spectrometer (JASCO NRS-2000), equipped with an Ar^+ laser with the wavelength of 514.5 nm and the laser power of 30 mW.

The hydroxyl contents were measured by FTIR method. Infrared spectra were measured using the Jasco MFT-2000 micro-sampling FTIR spectrometer. The measurements were carried out using a tungsten light source, Ge-coated KBr beam-splitter, and a high-sensitivity, wide-band MCT detector. Several hundred scans were accumulated for each spectrum with a 1-cm^{-1} resolution. During the measurements, the microscope was not purged with a stream of free gas. The effect of the absorbed water on the sample surface was found to be negligible by measuring samples with different thicknesses. Background corrections of the absorbance spectra were carried out by a spline polynominal fit to the baseline defined by points outside the hydrohyl-stretching region. We used unpolarized radiation to measure the H_2O contents. The H_2O contents were obtained by standard averaging the absorbance measured on several sample sections.

Micro-FTIR spectra were obtained from double-polished thin sections (40–100 μm) of polycrystalline aggregates of wadsleyite/ringwoodite with minor garnet, situated on a KBr plate. The concentrations of hydroxyl groups were determined by integrating absorption bands using the calibration of the extinction coefficient by Paterson (1982).

Results

Phase relations

The compositions of major DHMS produced at pressures above 10 GPa are presented in Fig. 1. This diagram shows that in pyrolite with low content of H_2O (e.g., 2 wt%) the phases A, E, chondrodite and superhydrous B can exist only with Mg_2SiO_4 polymorphs, olivine, wadsleyite and ringwoodite at pressures and temperatures in the upper mantle and the transition zone conditions. Additionally, superhydrous phase B and phase G/D/F can coexist with periclase and Mg-perovskite in the lower mantle. In the system, pyrolite

Table 2 Experimental results. *Cen* clinoenstatite; *Cpx* Clinopyroxene; *Ol* olivine; *Gt* garnet; *Wd* wadsleyite; *Rw* ringwoodite; *SuB* superhydrous phase B; *Mg-Pv* Mg-perovskite; *Ca-Pv* Ca-perovskite; *Pc* periclase; *CF* Al-rich phase with Ca-ferrite structure (Irifune and Ringwood 1993; Akaogi et al. 1999); *fl* vapour or fluid

Run no.	Pressure (GPa)	Temp. (°C)	Time (h)	Phase assemblage
K-67	10.0	900 (10)	24	Phase E, Ol, Cpx, Gt, Cen
K-53	10.0	1000 (10)[a]	10	Phase E, Ol, Cpx, Gt, fl
K-54	10.0	1200 (10)	6	Ol, CPx, Gt, fl
K-51	12.0	900 (10)[a]	24	Phase E, Wd, Gt, Cpx
K-56	12.0	1050 (10)[a]	10	Phase E, Wd, Gt, Cpx
K-55	14.0	850 (10)[a]	20	Phase E, Wd, Gt, Cpx
K-57	14.0	1000 (10)[a]	20	Wd, Gt, Cpx
K-59	16.0	850 (10)[a]	24	Phase E, Wd, Gt, Cpx
K-8	16.0	1200 (10)	5	Wd, Gt, Cpx, fl
K-1	16.0	1400 (10)	3	Wd, Gt, Cpx, fl
K-66	17.0	950 (10)	24	Wd, Gt, Cpx, fl
K-24	18.5	1000 (10)	8	SuB, Rw, Gt, fl
K-9	18.5	1200 (40)	3	Wd, Gt, Cpx, fl
K-6	18.5	1400 (10)	3	Wd, Gt, fl
K-52	20.0	1000 (10)[a]	20	SuB, Rw, Gt, Ca-Pv
K-115	21.5	1000 (10)[a]	20	SuB, Rw, Gt, Ca-Pv
K-108	21.5	1200 (10)	3	Rw, Gt, Ca-Pv, fl
K-113	24.5	1000 (40)	9	SuB, Mg-Pv, Ca-Pv, Rw, (CF)
K-119	25.0	1000 (10)[a]	20	SuB, Mg-Pv, Ca-Pv, Gt
K-105	24.5	1200 (10)	4	SuB, Mg-Pv, Ca-Pv, Gt
K-101	24.0	1400 (10)	3	Mg-Pv, Ca-Pv, Gt, Pc, fl

[a] These experiments were initially heated at 1200 °C for 2 h. Phases in parentheses are probably metastable at the indicated conditions

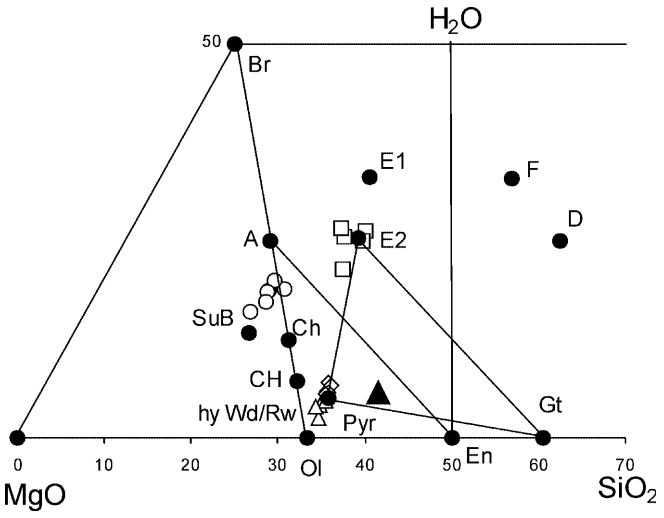

Fig. 1 Ternary diagram showing the composition of the dense magnesium silicate phases. *A* phase A; *E*1 and *E*2 phase E after Kanzaki et al. (1991) and Frost (1999), respectively; *Ch* chondrodite; *CH* clinohumite; *SuB* superhydrous phase B; *D* phase D (Frost and Fei 1998); *F* phase F (Kanzaki 1991); *Br* brucite; *Ol* olivine; *Wd*/*Rw* hydrous wadsleyite/ringwoodite ($H_2O = 2$ wt%); *Pyr* starting composition of pyrolite with 2 wt% of H_2O. Compositions of the phases analyzed in this study: *squares* phase E; *open circles* superhydrous phase B; *diamonds* hydrous wadsleyite; *open triangles* hydrous ringwoodite. The H_2O contents were estimated from the lower totals in the EPMA analyses, with an uncertainty of 2 wt% in DHMS and less than 0.7 wt% in Wd/Rw, and from FTIR in some wadsleyite/ringwoodite. Phase A can exist in pyrolite with 2 wt% of H_2O with olivine, as indicated by the phase A–enstatite join. Typical lower temperature assembly of Wd + Gt + phase E is joined as triangle

with ~2 wt% of H_2O, the maximum solubility of H_2O in hydrous Mg_2SiO_4 is 3.0 wt%. The theoretical limit for the solubility of H_2O in wadsleyite is close to this value (3.1 wt%), which is also consistent with experimentally obtained highest H_2O contents in wadsleyite by Inoue et al. (1995); however, solubility of H_2O in ringwoodite was found to be lower, up to ~2.7 wt% according to data by Kohlstedt et al. (1996).

Experimental conditions and the results are summarized in Table 2 and Fig. 2. Several hydrous phases were observed with increasing pressure. Phase E, $Mg_{2.3}Si_{1.25}H_{2.4}O_6$, is stable at 10 GPa and 900–1000 °C. Its modal amount at 900 °C is much higher than at 1000 °C (12 ± 3 and 3 ± 1 modal percent, respectively), and it coexists with clinoenstatite at 900 °C (Fig. 3A,B). Therefore, we suppose the reaction E + Cen = Fo + H_2O with a steep negative slope to the pressure axis, presuming the absence of clinoenstatite at higher temperature after Litasov and Ohtani (2002).

Phase E was also observed in the low-temperature experiments at 12–16 GPa to coexist with wadsleyite (Fig. 3D). At these pressures, phase E usually occurs as an interstitial phase between grains of other minerals. Phase E is not stable at 14 GPa and 1000 °C (Fig. 3E). Superhydrous phase B, $Mg_{10}Si_3O_{14}(OH)_4$, is stable at 18 GPa and below 1100 °C and it remains as a major hydrous phase up to 25 GPa. At 25 GPa superhydrous phase B is stable to about 1300 °C. It forms rounded or elongated grains in the range of 5–20 μm in size.

Mg-perovskite, periclase and ringwoodite were detected at 24.5 GPa and 1000 °C in one sample. Superhydrous phase B was detected at 24.5 GPa and 1200 °C, coexisting with the Mg-perovskite, Ca-perovskite, garnet and Al-rich phase (which could be a possible metastable phase). The Al-rich phase is NAL or CF (calcium ferrite structured phase: Akaogi et al. 1999; 2002) similar to that reported by Irifune and Ringwood (1993) in a

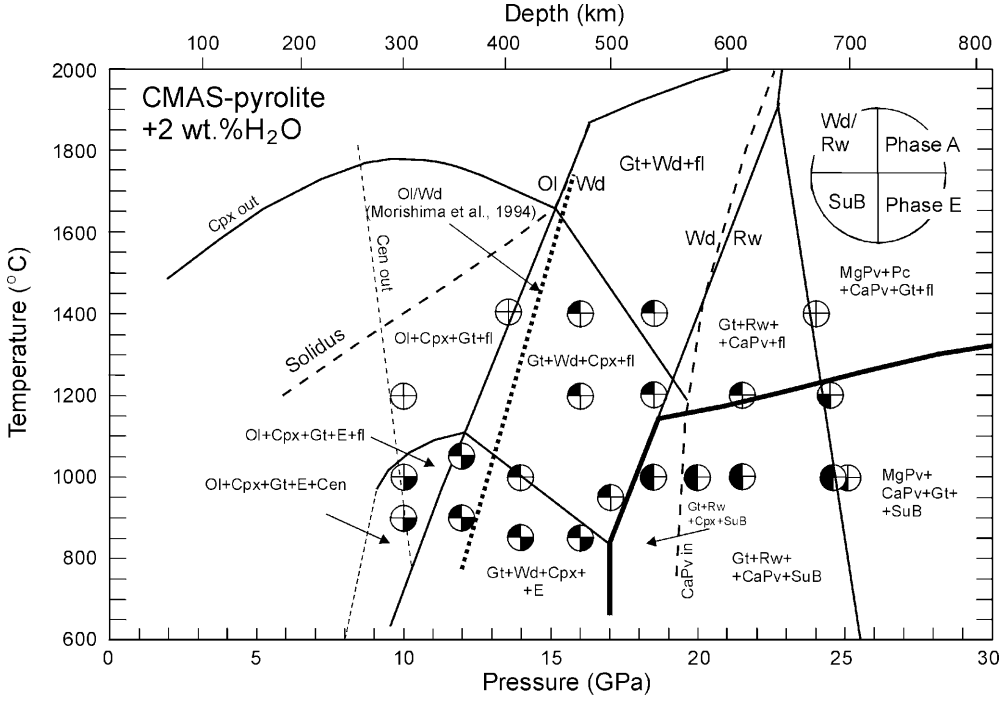

Fig. 2 Phase relations in the system CaO–MgO–Al_2O_3–SiO_2–pyrolite with 2% H_2O. *Solidus line* is after Litasov and Ohtani (2002). The wadsleyite–ringwoodite transition boundary is after Suzuki et al. (2000). Symbols are defined as follows: *Ol* olivine; *Cpx* clinopyroxene; *Cen* clinoenstatite; *Gt* garnet; *Wd* wadsleyite (modified spinel Mg_2SiO_4); *Rw* ringwoodite (spinel Mg_2SiO_4); *MgPv* Mg-perovskite; *CaPv* Ca-perovskite; *Pc* periclase; *SuB* superhydrous phase B; *fl* fluid. Stability of Ca-perovskite, clinopyroxene and clinoenstatite above 1400 °C is from Litasov and Ohtani (2002) and Asahara and Ohtani (2001). *Thick bold lines* confine the stability field of superhydrous phase B

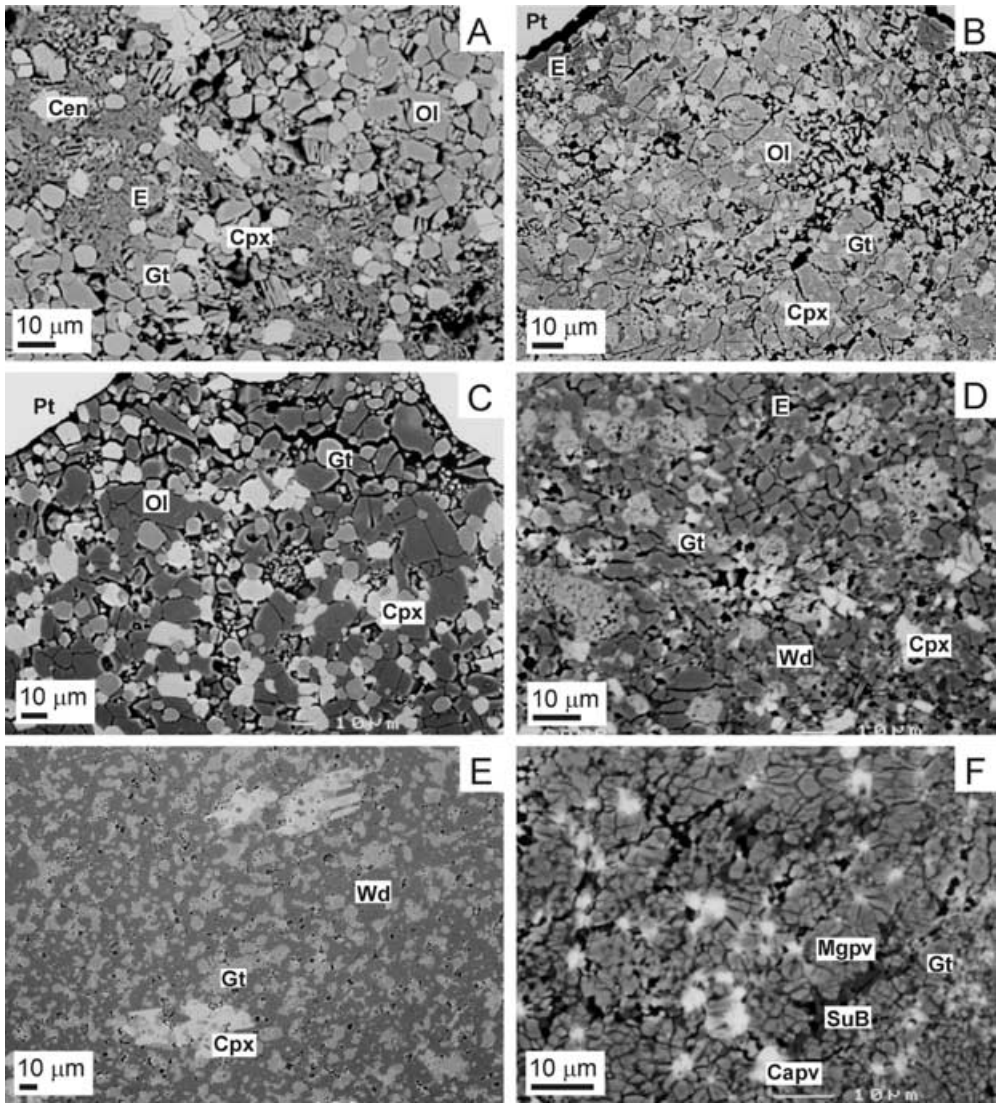

Fig. 3A–F BEI of run products. **A** Sample K-67 (10 GPa, 900 °C), modal amount of phase E is 12%. **B** Sample K-53 (10 GPa, 1000 °C), garnet segregates to porous patches, modal amount of phase E is 3%. **C** Sample K-54 (10 GPa, 1200 °C), Ol–Gt–Cpx aggregates with distinct fluid/melt-bearing patches. **D** Sample K-55 (14 GPa, 850 °C), lowest temperature run providing lack of disequilibrium microstructures. **E** Sample K-57 (14 GPa, 1000 °C), absence of phase E. **F** Sample K-119 (25 GPa, 1000 °C), high-pressure run, containing minor garnet and interstitial superhydrous phase B. Abbreviations: *Ol* olivine; *Cpx* clinopyroxene; *Cen* clinoenstatite; *E* phase E; *Gt* garnet; *Wd* wadsleyite; *Mgpv* Mg-perovskite; *Capv* Ca-perovskite; *SuB* superhydrous phase B

MORB composition and by Oguri et al. (2000) in the pyrope composition at 27 GPa.

Hydrous wadsleyite was observed at 12 GPa and 1050 °C. This indicates an expansion of the stability field of wadsleyite to lower pressures. Ringwoodite was found stable at 18.5 GPa and 1000 °C.

Fluid-bearing patches composed mostly of fine-grained crystals of majorite garnet were often found in the samples at temperatures of 1200–1400 °C and pressures between 16 and 20 GPa. We did not observe such segregations in some runs at 800–1050 °C, such as K-56 and K-55, containing phase E, and in runs K-119 and K-105 at pressures of 24–25 GPa and temperatures of 1000–1200 °C, containing superhydrous phase B.

Mineral chemistry and the H_2O content in wadsleyite and ringwoodite

Selected compositions of the phases from the experiments are listed in Table 3. Most of the phases, except garnet, show limited compositional variations. Phase E has the composition $Mg_{2.12–2.38}Al_{0–0.15}Si_{1.16–1.24}H_{2.4}O_6$. Superhydrous phase B contains significant amounts of Al_2O_3: about 0.7 wt% at 18.5 GPa and higher at 25 GPa, 1.9 wt% at 1200 °C and 4.7 wt% at 1000 °C.

The content of majorite component in garnet increases progressively with pressure. Al_2O_3 content of the garnet decreases from 20–22 wt% at 10 GPa to 7–10 wt% at 16–18 GPa. However, garnet coexisting with Ca-perovskite at 20 GPa and with Mg-perovskite at 25 GPa has shown once more a low content of majorite component and contains 20–22 wt% Al_2O_3. This is consistent with some previous results (Hirose 2002) and related data at high temperature reported by Litasov and Ohtani (2002).

Olivine has near-stoichiometric composition. However, the Mg/Si ratio of wadsleyite and ringwoodite is lower than 2.0, suggesting incorporation of H_2O. The H_2O contents in wadsleyite and ringwoodite estimated by FTIR method, and the Mg/Si ratio by EPMA, are

shown in Tables 3 and 4. Typical FTIR spectra of wadsleyite and ringwoodite are shown in Fig. 4. The H_2O contents in wadsleyite were found to be lower at 18.5 GPa than those at 16 GPa and at the same temperatures (Table 4). This could have important implications concerning heterogeneity in the water distribution in the transition zone, although the pressure dependence of the H_2O solubility in wadsleyite was not detected in previous experiments under water-saturated conditions (Inoue et al. 1995; Kohlstedt et al. 1996). Thus, further experiments may be needed to confirm this possibility.

Discussion

The stability of hydrous phases in the pyrolitic mantle

Reviews of the physical properties and the terminology of different dense hydrous magnesian silicates were made by several authors (Gasparik 1993; Frost 1999; Ohtani et al. 2001). They summarized that superhydrous phase B could be the same as phase C of Ringwood and Major (1967) and suggested the identity of the phases G, D and F. As was mentioned earlier, the major hydrous phases possibly stable in the pyrolite mantle compositions with increasing pressure are serpentine and chlorite, phase A, chondrodite, clinohumite, phase E, superhydrous phase B and phase G (Yamamoto and Akimoto 1977; Akimoto and Akaogi 1980; Kanzaki 1991; Kawamoto et al. 1995; Schmidt and Poli 1998; Frost 1999; Ohtani et al. 2000). We found that the stability fields of hydrous phases in the pyrolite mantle with ~2 wt% of H_2O are generally consistent with those determined via the simple $MgO–SiO_2–H_2O$ system or in a water-saturated primitive mantle composition, but several important differences are observed.

Phase A is stable in different systems from 3 to 17 GPa and its stability expands to the temperature of 1100 °C near 11 GPa (Pawley and Wood 1996; Frost 1999). It forms by the reaction of Fo + H_2O = Phase A + En at 8 GPa and 800 °C (Luth 1995) or by the breakdown of antigorite at 6 GPa and 600 °C (Ulmer and Trommsdorff 1995; Komabayashi et al. 2002). Phase A was not detected in this study, but was detected at 10 GPa and below 900 °C, together with phase E, clinohumite and enstatite by Kawamoto et al. (1995). The data on the stability of phase A, chondrodite and clinohumite (Yamamoto and Akimoto 1977; Akimoto and Akaogi 1980; Luth 1995; Wunder 1998; Stalder and Ulmer 2001; Fig. 5) show that the assemblage of phase A + olivine (+ gt + cpx + cen) could be stable at 7–10 GPa and below 800 °C. Obviously, in a system with low amount of H_2O, phase A plays a less important role in the upper mantle assemblages.

Phase E was observed in the system Mg_2SiO_4 + 20 wt% H_2O at 13–17 GPa and 800–1000 °C (Kanzaki 1991). The stability field of phase E partially overlaps with wadsleyite. At low temperatures wadsleyite can accommodate up to 3 wt% of H_2O (Inoue et al. 1995). Phase E is not supposed to be stable when wadsleyite is undersaturated with H_2O (Frost 1999). We found phase E coexisting with olivine at 10 GPa and 900–1000 °C, and with wadsleyite at 12 GPa and below 1050 °C, and at 16 GPa and 850 °C (Fig. 1). At 14–17 GPa and 1000 °C, we have no hydrous phases other than wadsleyite. Wadsleyite can accommodate up to about 3.0 wt% of H_2O (estimated from the analysis total) in the samples quenched at 14 GPa and 950–1000 °C. At 12–16 GPa, phase E coexists with wadsleyite below 900–950 °C (Fig. 1) in spite of wadsleyite being able to preserve more than 2 wt% of water. Thus, we can conclude that in this pressure range and below 950 °C the assemblage of wadsleyite + phase E is more stable than the wadsleyite phase only. In any case, wadsleyite is a major hydrous phase at 12–16 GPa in the pyrolite + 2 wt% H_2O system. We find a gap in the stability of the DHMS phases (i.e., phase E or super B) in this pressure range (Fig. 2). This breach may be explained by the higher solubility of H_2O in wadsleyite than in olivine or ringwoodite.

Superhydrous phase B coexisting with stishovite at pressures of 16–24 GPa and temperatures between 800 and 1400 °C was recognized by Gasparik (1990, 1993) with the starting composition with Mg/Si = 1.5 and 3.6 wt% of H_2O. In the experiments containing more H_2O, superhydrous phase B was observed coexisting with phase G/D at pressures of 16–24 GPa and temperatures of 900–1500 °C (Ohtani et al. 1995; Frost and Fei 1998). Limited H_2O solubility in ringwoodite stabilizes superhydrous phase B in pyrolite + 2 wt% of H_2O at 18–24 GPa. Superhydrous phase B was observed at the temperature below 1100 °C at 18.5 GPa and below 1300 °C at 25 GPa.

Other hydrous phases, suggested to be stable in the mantle, such as phase G or hydrous phase B, were not detected in the present experiments. However, according to Shieh et al. (1998), phase G can be synthesized at elevated pressures of 30 to 45 GPa from the serpentine bulk composition. Thus, we can predict that phase G is an important hydrous phase in the lower mantle at pressures above 30 GPa (Ohtani et al. 2001).

Water transport and storage in the mantle

Dense hydrous magnesium silicate phases (A, E, super B) cannot exist in pyrolite along a typical mantle geotherm due to their stability being restricted to the lower temperature and can occur only under the *P–T* conditions in the slabs descending into the mantle. At the normal mantle conditions, wadsleyite or ringwoodite are the major H_2O-bearing phases (Frost 1999; Ohtani et al. 2000, 2001). The transition zone, where these phases are stable, could be an important water reservoir in the Earth's mantle (e.g., Ohtani et al. 2001). The results of present experiments are consistent with these data (Fig. 6).

Table 3 Representative mineral compositions. See Table 2 for abbreviations

No.	P (GPa)	T (°C)	Phase	SiO_2 1σ	Al_2O_3 1σ	MgO 1σ	CaO 1σ	Total 1σ
K-67	10.0	900	Phase E	39.85	0.11	50.51	0.02	90.49
			Gt	47.08	20.16	26.53	6.38	100.2
			Cen	59.74	0.23	40.32	0.21	100.5
			CPx	54.56	0.24	20.34	23.07	98.21
K-53	10.0	1000	Phase E	39.57 (0.59)	2.88 (0.24)	45.94 (1.05)	0.04 (0.01)	88.43 (0.89)
			Ol	41.87	0.35	56.49	0.39	99.10
			Gt	44.40	21.96	25.35	7.47	99.18
			Cpx	55.10	0.24	20.08	23.41	98.83
K-54	10.0	1200	Ol	42.51	0.02	57.40	0.06	99.99
			Gt	45.29	21.16	25.71	7.13	99.29
			Cpx	55.99	0.24	19.55	23.98	99.76
K-51	12.0	900	Phase E	38.70 (0.93)	1.25 (0.59)	50.43 (0.69)	0.29 (0.12)	90.67 (1.03)
			Wd	42.75 (0.51)	0.33 (0.09)	54.02	0.12 (0.03)	97.22 (0.54)
			Gt	46.56	19.51	27.25	6.71	100.0
K-56	12.0	1050	Phase E	38.83 (0.76)	3.82 (0.23)	45.68 (1.25)	0.98 (0.12)	89.31 (0.54)
			Wd	43.08 (0.76)	0.28 (0.07)	54.26 (0.94)	0.01 (0.01)	97.63 (0.73)
			Gt	45.36	20.57	25.79	7.74	99.46
			Cpx	54.57	0.22	19.98	24.46	99.23
K-55	14.0	850	Phase E	37.54 (0.57)	0.41 (0.13)	50.28 (0.54)	0.21 (0.04)	88.44 (0.42)
			Wd	43.34 (0.79)	0.14 (0.05)	53.28 (0.91)	0.38 (0.15)	97.14 (0.89)
			Gt	45.23	19.92	26.21	8.12	99.48
			Cpx	54.49	0.83	20.37	23.81	99.50
K-36	14.0	950	Wd	43.30 (0.10)	0.42 (0.34)	53.45 (0.23)	0.17 (0.19)	97.34 (1.24)
			Gt	44.96	23.51	23.08	9.18	100.7
K-57	14.0	1000	Wd	43.01 (0.62)	0.21 (0.07)	53.63 (0.73)	0.09 (0.02)	96.94 (0.78)
			Gt	44.54	19.67	23.09	9.85	97.15
			Cpx	55.92	0.26	20.16	24.25	100.6
K-59	16.0	850	Phase E	36.52	0.17	50.61	0.58	87.88
			Wd	43.23(0.59)	0.45 (0.21)	52.26 (0.76)	0.69 (0.11)	96.63 (0.83)
			Gt	50.83	11.08	28.74	8.95	99.60
			Cpx	55.45	0.53	19.58	23.54	99.10
K-8	16.0	1200	Wd	43.29 (0.33)	0.33 (0.17)	53.95 (0.48)	0.13 (0.04)	97.70 (0.59)
			Gt	52.47	7.87	31.89	7.23	99.46
K-24	18.5	1000	SuB	30.59(1.19)	0.70 (0.11)	59.16 (1.61)	0.15 (0.03)	90.60 (0.89)
			Rw	43.23 (0.26)	0.53 (0.02)	53.79 (0.54)	0.38 (0.06)	97.93 (0.67)
			Gt	45.07	23.22	22.89	9.35	100.5
K-9	18.5	1200	Wd	43.03 (0.09)	0.20 (0.01)	54.48 (0.05)	0.08 (0.04)	97.79 (0.05)
			Gt	50.58	10.94	33.01	4.46	98.99
K-52	20.0	1000	SuB	33.14 (0.47)	1.52 (0.10)	55.32 (0.41)	1.12 (0.20)	91.10 (0.64)
			Rw	42.77 (0.73)	0.18 (0.08)	55.34 (0.85)	0.07 (0.02)	98.36 (0.73)
			Gt	46.67	21.05	26.24	6.23	100.2
K-115	22.0	1000	SuB	29.31 (0.88)	1.13 (0.41)	60.54 (0.72)	0.11 (0.04)	91.09 (1.02)
			Rw	43.27 (0.59)	0.21 (0.06)	54.54 (0.69)	0.17 (0.04)	98.19 (0.72)
			Gt	47.84	21.30	26.13	5.01	100.3
K-108	22.0	1200	Rw	43.17 (0.81)	0.01 (0.01)	55.75 (0.72)	0.07 (0.02)	99.00 (0.74)
			Gt	48.38	20.10	26.71	4.67	99.86
K-113	24.5	1000	SuB	27.24 (0.79)	1.79 (0.17)	61.31 (0.48)	0.08 (0.01)	90.42 (1.02)
			Rw	41.98 (1.05)	0.90 (0.24)	55.27 (0.99)	0.34 (0.10)	98.49 (1.12)
			Mg-Pv	60.00	0.76	40.17	0.75	101.7
K-119	25.0	1000	SuB	26.83 (0.44)	3.67 (0.20)	62.55 (0.89)	0.13 (0.04)	93.18 (0.72)
			Mg-Pv	59.86	0.81	39.94	0.58	101.2
			Ca-Pv	52.01	0.79	1.60	45.53	99.93
			Gt	45.47	21.44	29.34	3.23	99.48
K-105	24.5	1200	SuB	28.16 (0.50)	4.72 (0.37)	59.58 (0.50)	0.19 (0.03)	92.65 (1.18)
			Mg-Pv	59.47	1.32	39.01	1.07	100.9
			Gt	44.41	24.53	27.10	3.42	99.46
K-101	24.0	1400	Mg-Pv	56.23	1.02	40.82	1.79	99.86
			Gt	45.00	22.44	27.96	4.02	99.42

Significant amounts of water stored in serpentine in the cold descending slabs can be transported into the depth greater than 200 km. If the amount of water in the system is sufficient, the assemblage of phase A + Cen + Cpx is formed (Frost 1999). There is a complexity of following phase transformations at the boundary region between the shallow upper mantle and the transition zone. In the systems with low content of H_2O (2 wt%) phase E is possibly stable only in association with olivine at the depth of 250–350 km, and only under the P–T conditions in subducting slabs. In the case of cold subduction, phase E is pos-

Table 3 (Contd)

Si	Al	Mg	Ca	Total	O number	Mg/Si	H_2O–1	H_2O–2
0.976	0.003	1.843	0.001	2.823	3.8[a]	1.89	9.5	
0.801	0.405	0.673	0.116	1.996	3	0.84		
1.989	0.009	2.001	0.007	4.006	6	1.01		
1.989	0.010	1.105	0.901	4.006	6	0.56		
0.984	0.085	1.703	0.001	2.773	3.8	1.73	11.6	
0.991	0.010	1.993	0.010	3.004	4	2.01		
0.768	0.449	0.653	0.138	2.008	3	0.85		
1.996	0.010	1.084	0.909	3.999	6	0.54		
0.996	0.001	2.005	0.002	3.003	4	2.01		
0.781	0.431	0.660	0.132	2.004	3	0.85		
2.009	0.010	1.045	0.922	3.986	6	0.52		
0.948	0.036	1.842	0.008	2.834	3.8	1.94	9.3	
1.026	0.009	1.932	0.003	2.970	4	1.88	2.8	1.6
0.796	0.394	0.694	0.123	2.007	3	0.87		
0.961	0.112	1.685	0.026	2.783	3.8	1.75	10.7	
1.029	0.008	1.931	0.000	2.967	4	1.88	2.4	1.8
0.782	0.419	0.663	0.143	2.008	3	0.85		
1.978	0.009	1.079	0.950	4.017	6	0.55		
0.945	0.012	1.886	0.006	2.849	3.8	2.00	11.6	
1.040	0.004	1.905	0.010	2.958	4	1.83	2.9	2.3
0.782	0.407	0.675	0.150	2.015	3	0.86		
1.966	0.035	1.095	0.920	4.017	6	0.56		
1.036	0.012	1.906	0.004	2.958	4	1.84	2.7	2.3
0.767	0.474	0.587	0.168	1.996	3	0.77		
1.034	0.006	1.921	0.002	2.963	4	1.86	3.1	2.0
0.791	0.413	0.611	0.187	2.003	3	0.77		
1.993	0.011	1.071	0.926	4.001	6	0.54		
0.929	0.005	1.919	0.016	2.868	3.8	2.07	12.1	
1.042	0.013	1.878	0.018	2.951	4	1.80	3.4	2.6
0.878	0.226	0.740	0.166	2.009	3	0.84		
2.001	0.023	1.053	0.910	3.987	6	0.53		
1.033	0.009	1.918	0.003	2.963	4	1.86	2.3	2.0
0.904	0.160	0.819	0.133	2.016	3	0.91		
2.841	0.077	8.188	0.015	11.121	14	2.88	9.4	
1.029	0.015	1.909	0.010	2.963	4	1.85	2.1	2.0
0.771	0.469	0.583	0.171	1.995	3	0.76		
1.026	0.006	1.937	0.002	2.971	4	1.89	2.2	1.6
0.869	0.222	0.846	0.082	2.019	3	0.97		
3.040	0.165	7.563	0.110	10.878	14	2.49	8.9	
1.016	0.005	1.959	0.002	2.982	4	1.93	1.6	1.0
0.794	0.423	0.665	0.114	1.995	3	0.84		
2.718	0.124	8.367	0.011	11.220	14	3.08	8.9	
1.028	0.006	1.931	0.004	2.969	4	1.88	1.8	1.7
0.807	0.425	0.657	0.091	1.980	3	0.81		
1.019	0.000	1.961	0.002	2.981	4	1.92	1.0	1.0
0.819	0.402	0.674	0.085	1.980	3	0.82		
2.558	0.199	8.579	0.008	11.343	14	3.35	9.6	
0.998	0.025	1.958	0.009	2.990	4	1.96	1.5	0.6
0.989	0.015	0.987	0.013	2.004	3	1.00		
2.447	0.396	8.501	0.013	11.356	14	3.47	6.8	
0.991	0.016	0.985	0.010	2.002	3	0.99		
0.996	0.018	0.046	0.935	1.995	3	0.05		
0.774	0.432	0.745	0.059	2.010	3	0.96		
2.565	0.508	8.089	0.019	11.181	14	3.15	7.3	
0.988	0.026	0.966	0.019	1.999	3	0.98		
0.755	0.493	0.687	0.062	1.998	3	0.91		
0.953	0.020	1.031	0.033	2.037	3	1.08		
0.768	0.453	0.711	0.074	2.006	3	0.93		

[a] According to general formula of phase E (see text). H_2O–1, calculated from EPMA total. H_2O–2, calculated from Mg/Si ratio

sibly stable together with wadsleyite down to 450-km depths. In the hot subducting slabs wadsleyite can be the only hydrous phase at 350–500–km. In the depth range of about 520–550 km, we can expect the appearance of superhydrous phase B. It is possibly a major hydrous phase in the cold subducting slabs down to 700 km, i.e., the uppermost lower mantle (Fig. 6).

It is important to note that the stability field of wadsleyite expands to lower pressures in the presence of

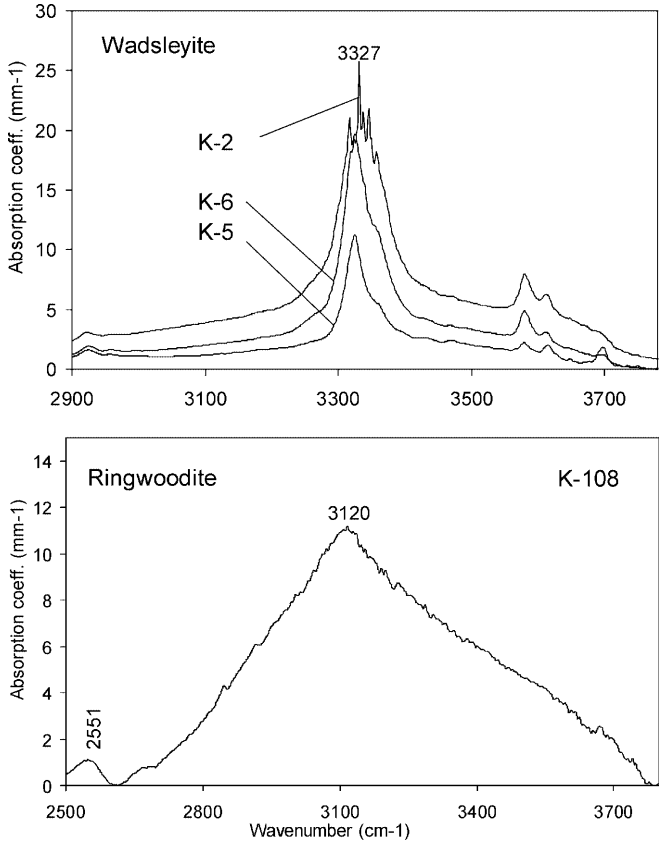

Fig. 4 Examples of FTIR spectra of Mg_2SiO_4 wadsleyite and ringwoodite. The *peak positions* are well correlated with data of Kohlstedt et al. (1996) and Bolfan-Casanova et al. (2000)

H_2O (Smyth and Frost 2002 and references therein). This can be important for the topography of the 410-km discontinuity, as well as for the temperature gradient

Table 4 Water content in wadsleyite and ringwoodite measured by FTIR

Run no	*P* (GPa)	*T* (°C)	Phase	Mg/Si	H_2O (wt%)
K-1	16.0	1400	wd	1.90	0.72 ± 0.17[b]
K-2[a]	16.0	1600	wd	1.93	0.70 ± 0.10
K-3[a]	17.0	1750	wd	1.97	0.33 ± 0.10[b]
K-6	18.5	1400	wd	1.90	0.46 ± 0.06
K-5[a]	18.5	1600	wd	1.94	0.29 ± 0.04
K-108	21.5	1200	rw	1.93	0.80 ± 0.20[b]

[a] Samples from Litasov et al. (2001)
[b] Calculated using broad bands (see Fig. 4)

near this boundary. Elevated sections of the 410-km discontinuity, which are not related to the subduction zones, should indicate H_2O enrichment. The data on the water solubility in wadsleyite also suggest that the uppermost transition zone could be enriched in H_2O (Fig. 6).

Recent data on the water solubility in Mg-perovskite, Ca-perovskite and magnesiowustite suggest that the lower mantle can accommodate H_2O in the nearly same total amount as in the transition zone (Murakami et al. 2002; Bolfan-Casanova et al. 2002). Superhydrous phase B and phase G are the major water carriers in the slabs descending into the lower mantle at 30–45 GPa (Shieh

Fig. 5A–D Experimental results on the stability of phase A in different systems. **A** The MgO–SiO_2–H_2O systems, *solid lines* are from Wunder (1998), *dashed lines* from Yamamoto and Akimoto (1977) and Luth (1995). **B** Serpentine composition, after Stalder and Ulmer (2001). **C** H_2O-saturated KLB-1 peridotite from Kawamoto et al. (1985). **D** Hydrous pyrolite represented in the present work and concluding compilation. *Fo* forsterite; *En* enstatite; *Chu* clinohumite; *Chn* chondrodite. See Fig. 2 for other abbreviations

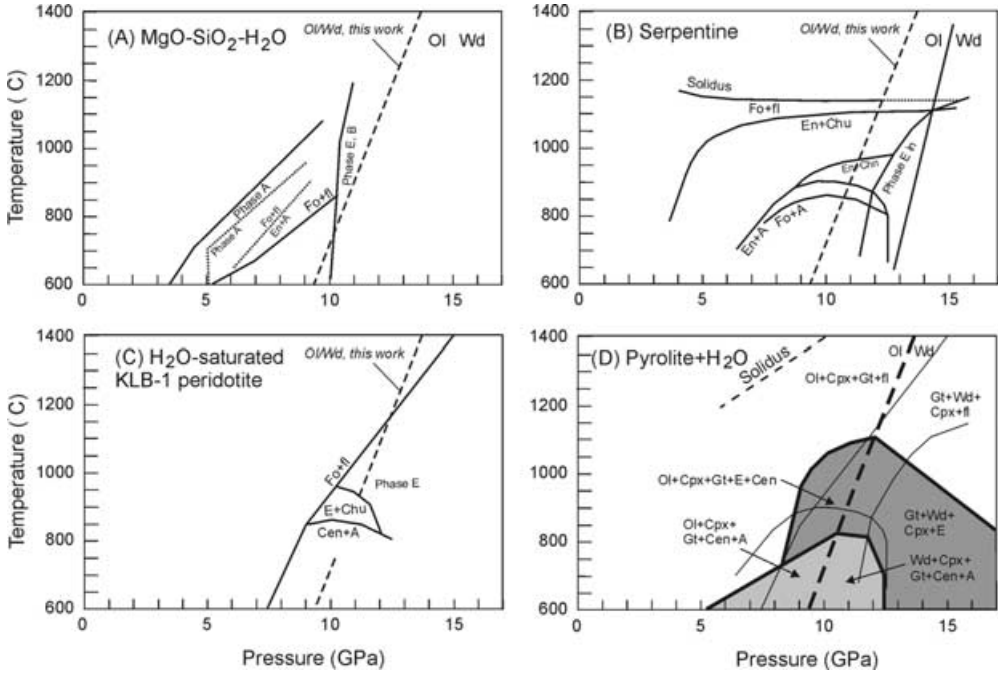

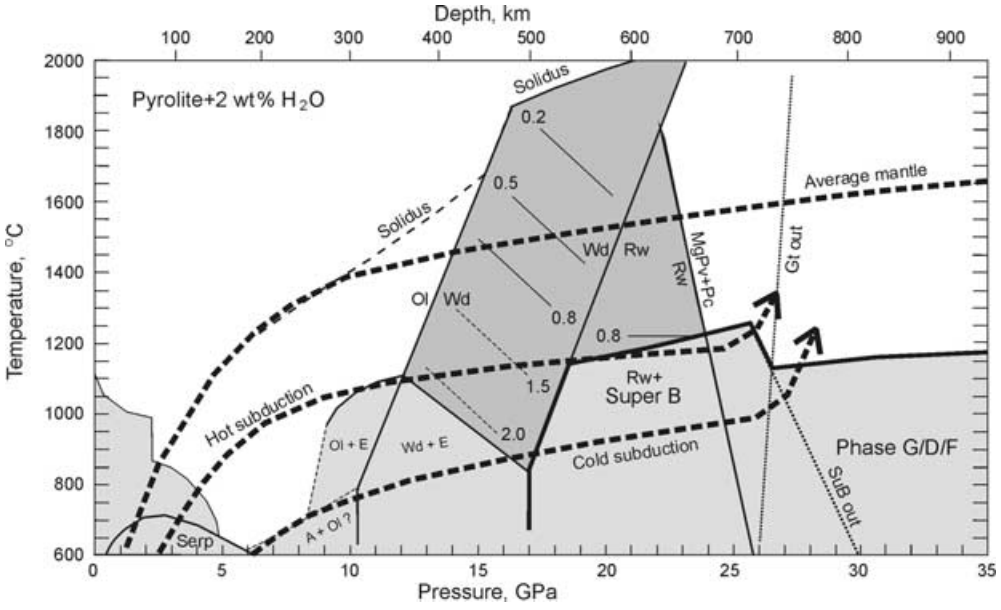

Fig. 6 Stability of the hydrous phases in the system CMAS-pyrolite + 2 wt% H_2O. The stability field of phase G (D/F) is after Shieh et al. (1998). The stability field of serpentine is after Ulmer and Trommsdorff (1995). Possible stability field of phase A + olivine (A + Ol + Cen + Cpx + Gt) are drawn using data presented in Fig. 5. Average mantle geotherm is from Akaogi et al. (1989). Subducting slab geotherms are after Thompson (1992) and Komabayashi et al. (2002). *Shaded areas* indicate the stability fields of the dense hydrous phases. See Fig. 2 for other symbols. Estimated water contents (wt%) of wadsleyite and ringwoodite are shown

1998; Ohtani et al. 2001). Therefore, they could supply water into the surrounding lower mantle.

Acknowledgements The authors are thankful to Y. Ito for the assistance with the EPMA measurement, A. Suzuki, T. Kubo and T. Kondo for technical help with the high-pressure experiments and Raman and X-ray diffraction measurements and C.R. Menako for technical support. K. Litasov thanks H. Taniguchi for his continuous encouragement and the Center for Northeast Asian Studies of Tohoku University and the Japanese Society for the Promotion of Science for the research fellowships. This work was partially supported by the Grant-in-Aid of Scientific Research of the Priority Area (B) of the Ministry of Education, Science, Sport, and Culture of the Japanese government (no. 12126201) to E. Ohtani.

References

Akaogi M, Ito E, Navrotsky A (1989) Olivine-modified spinel-spinel transitions in the system Mg_2SiO_4–Fe_2SiO_4: calorimetric measurements, thermochemical calculations, and geophysical application. J Geophys Res 94: 15671–15685

Akaogi M, Hamada Y, Suzuki T, Kobayashi M, Okada M (1999) High-pressure transitions in the system $MgAl_2O_4$–$CaAl_2O_4$: a new hexagonal aluminous phase with implication for the lower mantle. Phys Earth Planet Inter 115: 67–77

Akaogi M, Tanaka A, Kobayashi M, Fukushima N, Suzuki T (2002) High-pressure transformations in $NaAlSiO_4$ and thermodynamic properties of jadeite, nepheline, and calcium ferrite-type phase. Phys Earth Planet Int 130: 49–58

Akimoto S, Akaogi M (1980) The system Mg_2SiO_4–MgO–H_2O at high pressures and temperatures – possible hydrous magnesian silicates in the mantle transition zone. Phys Earth Planet Inter 23: 268–275

Asahara Y, Ohtani E (2001) Melting relations of the hydrous primitive mantle in the CMAS–H_2O system at high pressures and temperatures, and implications for generation of komatiites. Phys Earth Planet Inter 125: 31–44

Bolfan-Casanova N, Keppler H, Rubie D (2000) Water partitioning between nominally anhydrous minerals in the MgO–SiO_2–H_2O system up to 24 GPa: implications for the distribution of water in the Earth's mantle. Earth Planet Sci Lett 182: 209–221

Bolfan-Casanova N, Mackwell S, Keppler H, McCammon C, Rubie D (2002) Pressure dependence of H solubility in magnesiowustite up to 25 GPa: implications for the storage of water in the Earth's lower mantle. Geophys Res Lett 29: 10.1029/2001GL014457

Frost DJ (1999) The stability of dense hydrous magnesium silicates in Earth's transition zone and lower mantle. In: Fei Y, Bertka CM, Mysen BO (eds) Mantle petrology: field observations and high-pressure experimentation: a tribute to F.R. Boyd. Geochem Soc Spec Publ 6: 283–296

Frost DJ, Fei Y (1998) Stability of phase D at high pressure and high temperature. J Geophys Res 103: 7463–7474

Gasparik T (1990) Phase relations in the transition zone. J Geophys Res 95:15751–15769

Gasparik T (1993) The role of volatile in the transition zone. J Geophys Res 98: 4287–4299

Gasparik T (1996) Melting experiments on the enstatite–diopside join at 70–224 kbar, including the melting of diopside. Contr Mineral Petrol 124: 139–153

Hirose K (2002) Phase relations in pyrolitic mantle around 670-km depth: implications for upwelling of plumes from the lower mantle. J Geophys Res 107: 10.1029/2001JB000597

Inoue T, Yurimoto H, Kudoh Y (1995) Hydrous modified spinel, $Mg_{1.75}SiH_{0.5}O_4$: a new water reservoir in the mantle transition region. Geophys Res Lett 22: 117–120

Irifune T, Ringwood AE (1993) Phase transformations in subducted oceanic crust and buoyancy relationships at depths of 600–800 km in the mantle. Earth Planet Sci Lett 117: 101–110

Jagoutz E, Palme H, Baddenhausen H, Blum K, Cendales M, Dreibus G, Spettel B, Lorenz V, Wanke H (1979) The abundances of major, minor and trace elements in the Earth's mantle as derived from primitive ultramafic nodules. Proc 10th Lunar Planet Sci Conf, Tucson, Arizona, pp 2031–2050

Kanzaki M (1991) Stability of hydrous magnesium silicates in the mantle transition zone. Phys Earth Planet Inter 66: 307–312

Kawamoto T, Leinenweber K, Hervig RL, Holloway JR (1995) Stability of hydrous minerals in H_2O-saturated KLB-1 peridotite up to 15 GPa. American Institute of Physics Conference Proceedings 341: 229–239

Kohlstedt DL, Kepler H, Rubie DC (1996) Solubility of water in the α, β, and γ phases of $(Mg,Fe)_2SiO_4$. Contrib Mineral Petrol 123: 345–357

Komabayashi T, Omori S, Maruyama S (2002) A new petrogenetic grid for hydrous slab peridotite down to 800 km depth. Abst Superplume Int Workshop, TIT, Tokyo, pp 386–390

Litasov KD, Ohtani E (2002) Phase relations and melt compositions in CMAS–pyrolite–H_2O system up to 25 GPa. Phys Earth Planet Inter 134: 105–127

Litasov KD, Ohtani E, Taniguchi H (2001) Melting and solid phase relations in pyrolite–H_2O system at the transitional zone pressures. Geophys Res Lett 28: 1303–1306

Luth RW (1995) Is phase A relevant to the Earth's mantle. Geochim Cosmochim Acta 59: 679–682

McDonough WF, Sun SS (1995) The composition of the Earth. Chem Geol 120: 223–253

Morishima H, Kato T, Suto M, Ohtani E, Urakawa S, Utsumi W, Shimomura O, Kikegawa T (1994) The phase boundary between α- and β-Mg_2SiO_4 determined by in situ X-ray observation. Science 265: 1202–1203

Murakami M, Hirose K, Yurimoto H, Nakashima S, Takafuji N (2002) Water in Earth's lower mantle. Science 295: 1885–1887

Mysen BO, Ulmer P, Konzett J, Schmidt MW (1998) The upper mantle near-convergent plate boundaries. In: Hemley RJ (ed) Ultrahigh-pressure mineralogy, physics and chemistry of the Earth's deep interior. Rev Mineral 37: 97–138

OHara MJ (1968) The bearing of phase equilibria studies in synthetic and natural system on the origin and evolution of basic and ultrabasic rocks. Earth Sci Rev 4: 69–133

Oguri K, Funamori N, Uchida T, Miyajima N, Yagi T, Fujino K (2000) Post-garnet transition in a natural pyrope: a multi-anvil study based on in situ X-ray diffraction and transmission electron microscopy. Phys Earth Planet Inter 122: 175–186

Ohtani E, Shibata T, Kubo T, Kato T (1995) Stability of hydrous phases in the transitional zone and the uppermost part of the lower mantle. Geophys Res Lett 22: 2552–2556

Ohtani E, Mizobata H, Yurimoto H (2000) Stability of dense hydrous magnesium silicate phases in the system Mg_2SiO_4–H_2O and $MgSiO_3$–H_2O at pressures up to 27 GPa. Phys Chem Miner 27: 533–544

Ohtani E, Touma M, Litasov K, Kubo T, Suzuki A (2001) Stability of hydrous phases and water storage capacity in the transitional zone and lower mantle. Phys Earth Planet Inter 124: 105–117

Paterson MS (1982) The determination of hydroxyl by infrared absorption in quartz, silicate glasses and similar materials. Bull Mineral 105: 20–29

Pawley AR, Wood BJ (1996) The low-pressure stability of phase A, $Mg_7Si_2O_8(OH)_6$. Contrib Mineral Petrol 124: 90–97

Ringwood AE (1975) Composition and petrology of the Earth's mantle. McGraw Hill, New York, 630 pp

Ringwood AE, Major A (1967) High-pressure reconnaissance investigations in the system Mg_2SiO_4–MgO–H_2O. Earth Planet Sci Lett 2: 130–133

Schmidt MW, Poli S (1998) Experimentally based water budgets for dehydrating slabs and consequences for arc magma gemeration. Earth Planet Sci Lett 163: 361–379

Shieh SR, Mao HK, Hemley RJ, Ming LC (1998) Decomposition of phase D in lower mantle and the fate of dense hydrous silicates in subducting slabs. Earth Planet Sci Lett 159: 13–23

Smyth JR, Frost DJ (2002) The effect of water on the 410-km discontinuity: an experimental study. Geophys Res Lett 29: 10.1029/2001GL014418

Stalder R, Ulmer P (2001) Phase relations of serpentine composition between 5 and 14 GPa: significance of clinohumite and phase E as water carrier into the transition zone. Contrib Mineral Petrol 140: 670–679

Suzuki A, Ohtani E, Morishima H, Kubo T, Okada T, Terasaki H, Kato T, Kikegawa T (2000) In situ determination of the phase boundary between wadsleyite and ringwoodite in Mg_2SiO_4. Geophys Res Lett 27: 803–806

Ulmer P, Trommsdorff V (1995) Serpentine stability to mantle depths and subduction-related magmatism. Science 268: 858–861

Wunder B (1998) Equilibrium experiments in the system MgO–SiO_2–H_2O (MSH): stability fields of clinohumite-OH [$Mg_9Si_4O_{16}(OH)_2$], chondrodite-OH [$Mg_5Si_2O_8(OH)_2$] and phase A [$Mg_7Si_2O_8(OH)_6$]. Contrib Mineral Petrol 132: 111–120

Yamamoto K, Akimoto S (1977) The system MgO–SiO_2–H_2O at high pressure and temperatures. Stability field of hydroxyl-chondrodite, hydroxyl-clinohumite and 10 Å phase. Am J Sci 277: 288–312